Structural and dielectric relaxation behaviour of $Ba_{0.8}Sr_{0.2}Zr_{0.1}Ti_{0.9}O_3$ ceramic

Tanusree Mondal[1], Bishnu Pada Majee[1], Tapas Ranjan Middya[2], P M Sarun[1], *

[1]Functional Ceramics Laboratory, Department of Applied Physics, Indian School of Mines, Dhanbad – 826004, India
[2]Department of Physics, Jadavpur University, Kolkata 700 032, India.

Corresponding author's email: sarun.res@gmail.com.

Abstract. $Ba_{0.8}Sr_{0.2}Zr_{0.1}Ti_{0.9}O_3$ (BSZT) ceramic was prepared by conventional solid state reaction technique. The XRD pattern confirms single phase formation with cubic structure. The surface morphology was analysed by field emission scanning electron microscopy (FE-SEM). Detailed investigation of dielectric and electrical properties of the BSZT ceramic was done in the wide temperature (453K – 573K) and frequency range (40Hz – 5MHz). Dielectric studies of the compound revealed that dielectric parameters were strongly dependent on temperature and frequency. The complex impedance analysis confirms that the conduction of BSZT ceramic was mainly due to the grain in the lower temperature and with increasing temperature electrode effect was becoming prominent. The conductivity of the material was found to obey the power law.

1. Introduction

Barium titanate ($BaTiO_3$) based materials is always extensively studied for a wide variety of electrical properties and applications. After the discovery of the compound, several A-site and B-site isovalent modified $BaTiO_3$ (BT) is investigated. Moreover, several possible substitutions on both A-site and/or B-site in $BaTiO_3$ is an effective way to improve the properties such as lowering the transition temperature (T_c), increasing dielectric constant [1-3]. Barium strontium titanate, $(Ba,Sr)TiO_3$ (BST) is one of the promising candidate among the modified BT compound because of its high dielectric constant and low dielectric dissipation factor. It is also considerable as a suitable material for the application in microwave and millimeter range such as phase shifters, frequency agile filters, and tunable capacitors [4-6]. Whereas, $Ba(Zr,Ti)O_3$ (BZT) is a possible alternative to BST because of its enhanced chemical stability over $BaTiO_3$ due to the substitution of chemically more stable Zr^{4+} ion than Ti^{4+} onto B sites. $Ba(Zr,Ti)O_3$ compound is extensively studied with variation of Zr concentration for high dielectric constant [7-9]. Therefore, substitution of both Sr and Zr into $BaTiO_3$ may give desirable result. $BaZr_{0.1}Ti_{0.9}O_3$ is chosen as a host material due to high dielectric and piezoelectric properties among $Ba(Zr,Ti)O_3$ compound for substitution of Sr. However, temperature dependent dielectric and ferroelectric properties of Sr doped $BaZr_{0.1}Ti_{0.9}O_3$ is reported [10,11]. Most of the cases, $BaZr_{0.1}Ti_{0.9}O_3$ is formed with tetragonal phase, but a change in phase is observed with the variation of Sr concentration. The physical properties of the materials can significantly change the electrical properties of the compound. The physical properties depend upon chemical composition and microstructure of the materials.

In the present work, the dielectric and electrical properties of optimized single phase $Ba_{0.8}Sr_{0.2}Zr_{0.1}Ti_{0.9}O_3$ (BSZT) ceramic are investigated at low frequencies (40Hz-5MHz) in the range of temperature 453K – 573K.

2. Experimental

BSZT ceramic was prepared through conventional solid state technique. Stoichiometric mixtures of ingredients, $BaCO_3$, $SrCO_3$, ZrO_2 and TiO_2 (<99.9%) were mixed using an agate morter and pestle in acetone medium and subsequently calcined at temperature 1300°C for 4 h. The calcined powder was homogenized in acetone again and dried in an oven at 200°C for approximately 1 h. PVA (Poly Vinyl Alcohol) of 3 wt% was used as a binder with the calcined powder during the preparation of pellets, having of thickness ~1.2 mm and a diameter of 12 mm under a pressure of 175 MPa. The prepared pellets were sintered at 1350°C for 4 h in muffle furnace with an accuracy of ±1°C.

The crystal structure of the material was analysed by X-ray diffractometer (XRD) using Cu-Kα1 radiation (Bruker D8-Focus). FE-SEM (ZEISS Supra-55) was used to analyse the surface morphology of the samples. To perform dielectric characterization, the conducting silver paste was coated on both sides of the pellets and was cured at a 150°C for 2 h. Dielectric and impedance parameters of BSZT ceramic were studied as a function of temperature in the wide frequency range (40Hz - 5MHz) by using LCR meter (Hioki-3552).

3. Results and discussion

3.1. Structural characterization

The typical XRD pattern of the sintered sample is shown in the figure 1. All the peaks are indexed according to the standard X-ray pattern of the cubic $BaTiO_3$ (ICDD PDF-2 No. 74-1962). Lattice parameter of the sample is calculated by considering the cubic structural symmetry for the BSZT system by using the formula,

$$\frac{1}{d^2} = \frac{h^2 + k^2 + l^2}{a^2} \tag{1}$$

The calculated value of lattice parameter is α=b=c= 3.99Å which is good agreement with the standard data.

The inset of figure 1 shows FE-SEM image of the fractured surface of BSZT sample. The figure shows domain structure with “lamellar” and water-mark characters in FESEM image as indicated by circles. The grains having an irregular morphology and are distributed non-uniformly but with well define grain boundaries.

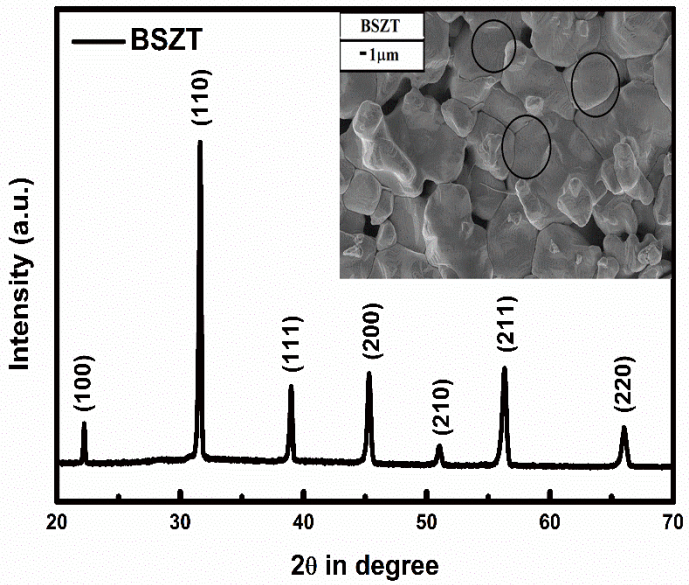

Figure 1. XRD pattern of BSZT ceramic. The inset shows FE-SEM image of BSZT.

3.2. Dielectric characterization

The complex dielectric permittivity is studied by using the formula $\varepsilon^* = \varepsilon'(\omega) - j\varepsilon''(\omega)$; (where, ε' is the real part of the permittivity, ε'' is the imaginary part or loss part with j =$\sqrt{-1}$). The following set of equation is used to obtain the values of ε' and tanδ,

$$\varepsilon'(\omega) = C_0(\omega)\frac{d}{A\varepsilon_0}, \quad (2)$$

$$\varepsilon''(\omega) = \varepsilon'(\omega)\tan\delta, \quad (3)$$

Where, d and A is the thickness and effective area of the sample, tanδ is the dissipative factor, δ the phase angle and $\omega=2\pi f$, is the angular frequency of the applied external electric field.

Figure 2(a) shows the logarithmic angular frequency ($\omega=2\pi f$) dependence variations of real part of complex dielectric permittivity ε' at 453K to 573K. ε' decreases with increasing frequency in the entire temperature range which is due to the inertia of dipoles to not to get polarized instantaneously with the application of electric field as dipoles are beginning to lag behind the field. The delay in response towards the applied field results in the loss which gives a dramatic decrease in ε'. At low frequency, free charge accumulation near grain boundaries causes higher value of dielectric constant, whereas, low dielectric constant at high frequency comes from grain. [12, 13]. At higher temperature, polarization occurs because of free movement of charge carriers through the crystal and thus ε' increases.

The variation of dielectric loss (tanδ) with frequency as a function of temperature is shown in figure 2(b). The variation of tanδ is also shows decreasing behaviour as similar to the dielectric constant of the sample which exhibit dispersion. At the lower frequency, due to the higher energy loss, tanδ value is high. But at the same time tanδ value become low in the higher frequency range for the low energy loss. The relaxation peaks are observed in the graph for tanδ attribute to the fact that hoping frequency of the charge carriers is approximately equal to frequency of the external applied field [14]. The peak position of tanδ shifts to higher frequency region with increasing temperature. The observed phenomenon suggests that charge carriers start to increase in the sample by thermal agitation.

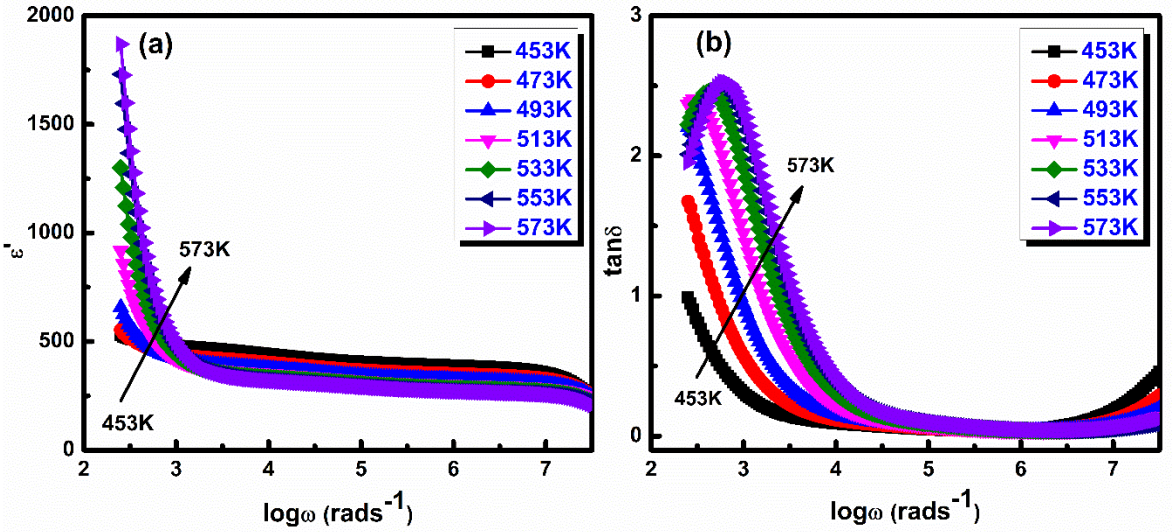

Figure 2. Variation of (a) ε′ and (b) tanδ with frequency at various temperatures for BSZT ceramic.

3.3. Impedance studies

Figure 3(a) and 3(b) exhibits the logarithmic angular frequency dependence of Z' and Z'' at different temperatures. Z' decreases continuously with increasing frequency as well as with temperatures and then turn out as frequency independent. The decrement in Z′ value results increment of ac-conductivity with the rise in both temperature and frequency in the material. The independent nature at higher frequency is due to the release of space charges. Z' is almost constant at higher temperatures (553K and 573K). The imaginary part of impedance loss spectrum (Z″) shows sharpe relaxation peaks in the higher temperatures. The average peak position shifts towards the high frequency side with the rise in temperature indicates that the grain resistivity of the material is decreasing. The broadening of peaks is also observed in Z″ with increasing temperature suggests the presence of temperature dependent relaxation process in the material.

Complex impedance spectroscopy is a useful tool to correlate the structural and electrical properties. Figure 3(c) shows Nyquist plot of BSZT ceramic. A single semi-circle arc is observed in BSZT ceramic for 453K, 473K and 493K temperatures and can be explained by an equivalent parallel resistance-capacitance (RC) circuits in an ideal case or the same can be modelled as resistance-constant phase element (R-CPE) network. This implies that the polarization mechanism in the compound arises mainly due to the grain for that particular temperatures. The intersection of the first semicircle with the Z′-axis gives the grain resistance (R_g) of the material. It is also observed that the first semicircle arc continues as another half semicircle with the further increment of the temperatures. The first semicircle arc at high frequencies is corresponds to grain, whereas, second one is for electrode effect at lower frequencies. However, semicircular arc become smaller with increasing temperature i.e the intercept point in the real axis shift towards the origin indicating the grain resistance of the sample decreased with increasing temperature. It also indicates that as the temperature increases, resistive properties of the sample is decreasing due to the formation of additional charge carriers by thermal agitation.

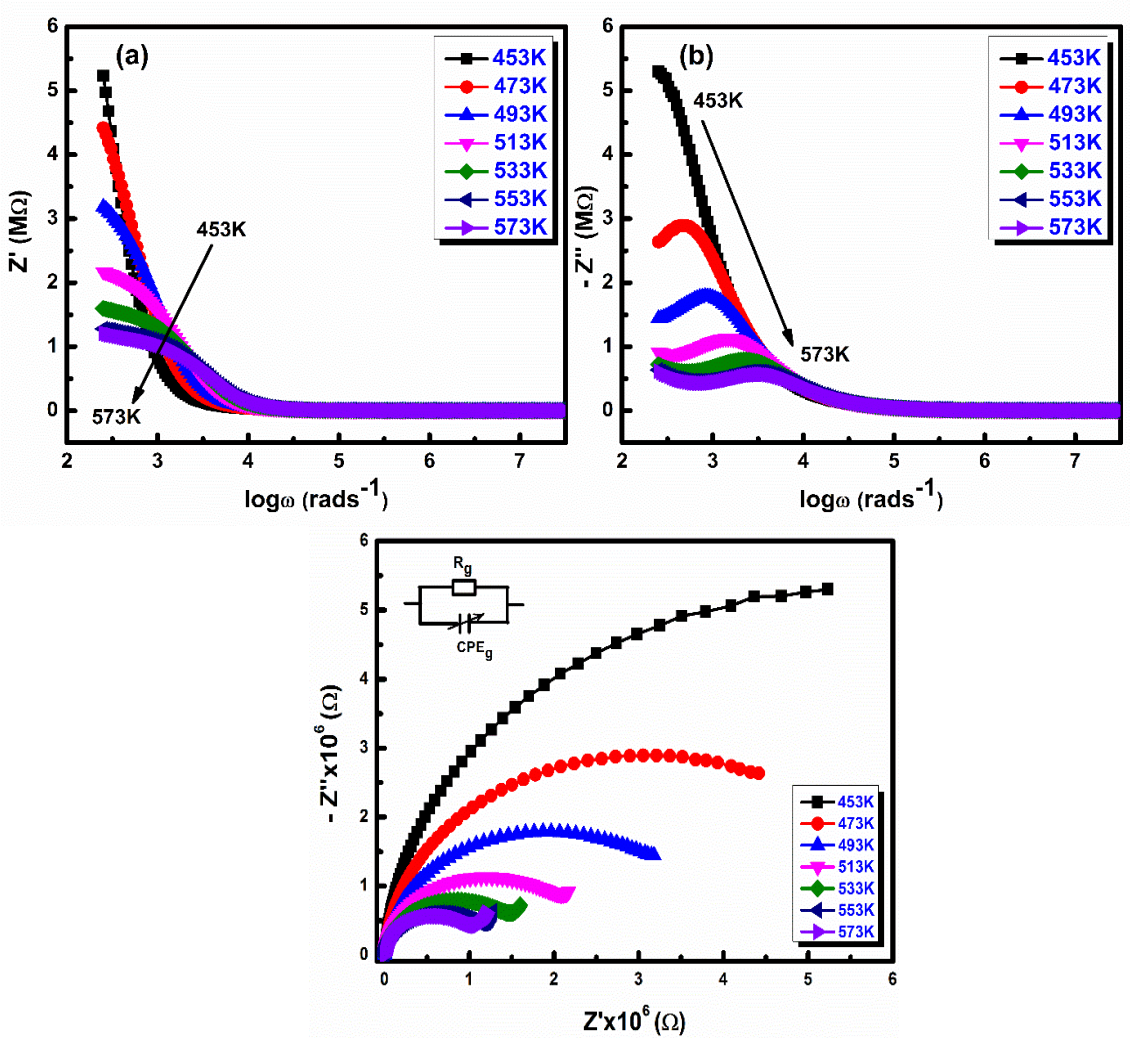

Figure 3. Variation of (a) real (Z′) and (b) imaginary part (Z′′) of impedance of BSZT ceramic as a function of frequency. (c) Nyquist plots of BSZT ceramic at different temperatures.

3.4. Modulus analysis

Modulus analysis is used to replot the impedance data and to find out the relaxation processes responsible for electrical conduction in the material. The complex modulus is calculated by the following relation:

$$M^* = 1/\varepsilon^*(\omega) = M' + jM'' \quad (4)$$

$$M' = \omega C_0 Z'' \text{ and } M'' = \omega C_0 Z' \quad (5)$$

where, ω is the angular frequency ($\omega = 2\pi f$) and C_0 is the geometrical capacitance. Figure 4(a) shows variation of real part of modulus as a function of angular frequency at different temperatures. A very low value of M′ is observed for the lower frequencies. But sigmoidal increment is observed with increasing frequency for all the temperature. The observed phenomena is due to short range mobility of charge carriers.

The variation of imaginary part of M′′ is shown by the figure 4(b) at the same temperatures. The height of maximum peak (M''_{max}) is found to be increased with increasing temperature. At the left side of peak maxima, the charge carrier can move for long time while, the motion of charge carrier is

confined in the right side frequencies of the peak. The peak in the M″ refers the existence of a hopping mechanism of the electrical conduction in the material.

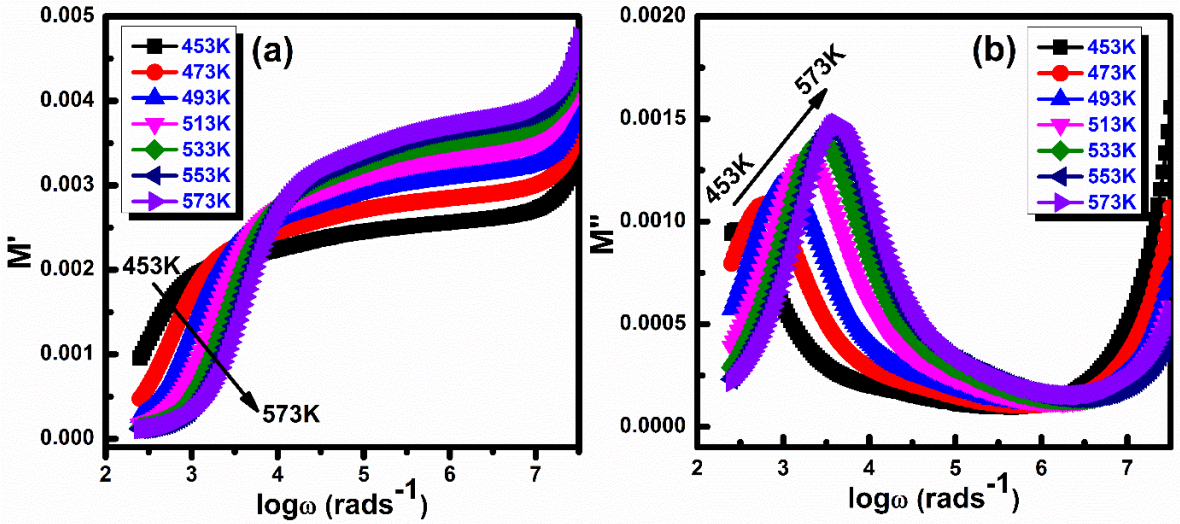

Figure 4. Variation of (a) real and (b) imaginary part of modulus with angular frequency of BSZT ceramic.

3.5. Conductivity study

Conductivity analysis gives the information about transport of charge carriers, i.e. electron/holes or cations/anions and their behavioural change as a function of temperature and frequency. The electrical conductivity of the sample can be expressed as:

$$\sigma = \omega\varepsilon_0\varepsilon'', \tag{6}$$

where, ω is the angular frequency, ε_0 is the dielectric permittivity in the vacuum and ε″ the imaginary part of complex dielectric permittivity (ε*).

The variation in conductivity of BSZT with angular frequency at different temperature between 453K to 573K is shown in figure 5. The observed low frequency plateau region in the figure represents frequency independent dc-conductivity (σ_{dc}) of the sample. At low frequencies, conductivity is found to be increased with increasing temperature. However, there is a shift of the frequency independent plateau region towards the high frequency side with increasing temperature. The total conductivity of the material at a given temperature can be fitted with Jonscher power law [15] expressed as:

$$\sigma = \sigma_{dc} + A\omega^n \tag{6}$$

Where, σ_{dc} is dc-conductivity, ω is applied angular frequency, A is frequency independent but temperature dependent parameter and n is the dimensionless term which varies from $0 \le n \le 1$. At higher frequency region, conductivity becomes almost temperature independent.

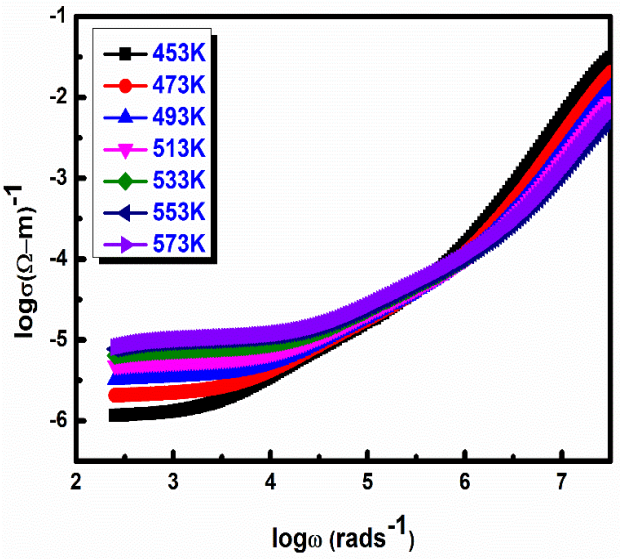

Figure 5. Variation of angular frequency dependence conductivity at different temperature.

Random diffusion of charge carriers via hopping gives rise to the observed frequency-independent conductivity at low frequencies while at higher temperatures more number of charge carriers are created due to the thermal agitation resulting in an increased conductivity.

4. Conclusion

The dielectric and electrical properties of $Ba_{0.8}Sr_{0.2}Zr_{0.1}Ti_{0.9}O_3$ ceramic were studied over a wide range of temperature and frequencies. The optimized single phase BSZT ceramic was successfully prepared through conventional solid state reaction method. The microstructural analysis shows water-mark and lamellar like domain structures of the sample. The complex impedance analysis suggests that the grains of the material were contributed on the conduction mechanism of the sample in lower temperatures whereas, with increasing temperature electrode effect become prominent. Modulus analysis reveals the presence of hopping mechanism of the conduction process in BSZT. The conductivity was analyzed on the basis of increment of mobility of free charges with increasing temperature and frequency.

Acknowledgments

Tanusree Mondal acknowledges the Indian School of Mines, Dhanbad, India for providing the Senior Research Fellowship (SRF).

References

[1] Shukai Y, Jerry F and Li L 2012 *J. Alloys Comp.* **541** 402.
[2] Reddy S B, Rao K P and Rao M S R 2011 *J. Alloys Compd.* **509** 1270.
[3] Jha A P and Jha A 2013 *Curr. Appl. Phys.* **13** 1419.
[4] Tiwari V S, Singh N and Pandy D 1995 *J. Phys. Condens. Matter.* **7** 1460.
[5] Suasmoro S, Pratapa S, Hartanto D, Setyoko D and Dani U M 2000 *J. Eur. Ceram. Soc.* **20** 314.
[6] Tagantsev A K, Sherman V O, Astafiev K F, Venkatesh J and Setter N 2003 *J. Electroceram.* **11** 5.
[7] Cristina E C, Maria T B, Vincenzo B and Liliana M 2011 *J. Appl. Phys.* **110** 114110.
[8] Zixiong S, Yongping P, Zijing D, Yao H, Xiaoyan L and Peikui W 2014 *Ceram. Int.* **40** 3594.
[9] Mahajan S, Thakur O P, Prakash C and Sreenivas K 2011 *Bull. Mater. Sci.* **34** 1489.
[10] Chan N Y, Choy S H, Wang D Y, Wang Y, Dai J Y and Chan H L W 2014 *J Mater Sci: Mater Electron* **25** 2594.
[11] Reddy S B, Rao K P and Rao M S R 2007 *Appl. Phys.* A **89** 1015.

[12] Hsiao Y J, Chang Y H, Fang T H and Chang Y S 2005 *Appl. Phys. Lett.* **87** 142906.
[13] Prasad A and Basu A 2012 *Mater. Lett*. **66** 3.
[14] Dutta A, Bharti C, Sinha T P 2008 *Mater. Res. Bull.* **43** 1246.
[15] Jonscher A K 1977 *Nature* **267** 673.